

**AUTHOR QUERY FORM**

	<p><b>Journal:</b> JEST</p> <p><b>Article Number:</b> 3972</p>	<p><b>Please e-mail or fax your responses and any corrections to:</b></p> <p><b>E-mail:</b> <a href="mailto:corrections.esch@elsevier.sps.co.in">corrections.esch@elsevier.sps.co.in</a></p> <p><b>Fax:</b> +31 2048 52799</p>
---	--	--

Dear Author,

Please check your proof carefully and mark all corrections at the appropriate place in the proof (e.g., by using on-screen annotation in the PDF file) or compile them in a separate list. Note: if you opt to annotate the file with software other than Adobe Reader then please also highlight the appropriate place in the PDF file. To ensure fast publication of your paper please return your corrections within 48 hours.

For correction or revision of any artwork, please consult <http://www.elsevier.com/artworkinstructions>.

Any queries or remarks that have arisen during the processing of your manuscript are listed below and highlighted by flags in the proof. Click on the 'Q' link to go to the location in the proof.

<b>Location in article</b>	<b>Query / Remark: <a href="#">click on the Q link to go</a> Please insert your reply or correction at the corresponding line in the proof</b>
<p><a href="#">Q1</a></p> <p><a href="#">Q2</a></p>	<p>Please confirm that given names and surnames have been identified correctly.</p> <p>Please check whether the designated corresponding author is correct.</p> <div data-bbox="416 1868 979 1970" style="border: 1px solid black; padding: 5px; margin-top: 20px;"> <p style="color: red;">Please check this box if you have no corrections to make to the PDF file</p> <input data-bbox="868 1885 940 1949" type="checkbox"/> </div>

Thank you for your assistance.

---

**Highlights**

---

► Analysis of ring interaction mechanisms when lining is subjected to design loads. ► Significant increases of lining stiffness caused by so called coupling effects. ► Influence zone determined by soft ground conditions and high ovalization loads. ► Coupling can produce increments of the internal bending forces over 150%. ► Recommendations about usual design practices based on isolated ring models.

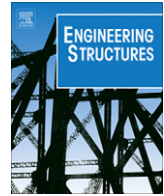
---



Contents lists available at SciVerse ScienceDirect

# Engineering Structures

journal homepage: [www.elsevier.com/locate/engstruct](http://www.elsevier.com/locate/engstruct)



## Three dimensional structural response of segmental tunnel linings

**Oriol Arnau\***, **Climent Molins**

Department of Construction Engineering, Universitat Politècnica de Catalunya (UPC), Jordi Girona 1-3, C1, 08034 Barcelona, Spain

### ARTICLE INFO

**Article history:**  
Received 22 September 2011  
Revised 18 April 2012  
Accepted 1 June 2012  
Available online xxx

**Keywords:**  
Segmental tunnel linings  
Coupling effects  
3D response  
Numerical simulation  
Nonlinear analysis

### ABSTRACT

The particular configuration of segmental tunnel linings produces that its structural response in front of usual design loads could present a significant three dimensionality due to the structural interaction between adjacent rings (coupling effects). The present paper studies the phenomena associated to coupling effects, determines the main involved parameters and analyzes their influence on a real lining structural response by means of a 3D numerical model. The comparison with the usual plane models currently employed in linings designs provide significant conclusions about the coupling effects implications and the conditions in which become more relevant.

© 2012 Published by Elsevier Ltd.

### 1. Introduction

The evolution and improvement of the modern tunnel boring machines (TBMs) allows the construction of tunnels at an increasing range of depths, dimensions and ground conditions. As the TBM advances, a segmental lining composed of multiple adjacent concrete rings is continuously placed (Fig. 1). This segmental lining provides both the structural capacity to resist the ground and water pressures and the necessary reaction frame to push the TBM ahead. Each ring comprises a certain number of concrete segments, creating a multiple-hinged structure that presents a complex structural behavior [1–3]. The staggered configuration of the joints (masonry layout, Fig. 1) is commonly employed with the main objective of minimizing the sealing problem when four corners of the segments coincide (cross joints) [2,4].

Usual tunnel conditions imply a nearly hydrostatic pressure that smoothly varies along the tunnel course. The longitudinal homogeneity of the ground produce that adjacent rings present the same load scheme and the consequent similar deformations that should not produce significant three dimensional responses. Despite that, the existence of coupling effects between adjacent rings is commonly accepted for linings with the staggered configuration of the joints. It is assumed that part of the bending force of a ring is transferred to the adjacent ones by means of the shear capacity of the circumferential joints (between adjacent rings) (Fig. 2). Initial attempts to consider this interaction were based on the inclusion of a transfer ratio of bending forces ( $\zeta$ ) in the

analytical formulations employed to determine the member forces in segmental linings [5,6] (Fig. 2). The main handicap is the selection of its value according to the particularities of the tunnel that is being designed. JSCE [5] recommends a value of  $\zeta$  between 0.3 and 0.5 based on the experience and the experimentation. Despite that, the usual design practice is based on the isolated ring models, maybe due to the lack of contrasted knowledge about the real coupling effects of rings.

The structural interaction between adjacent rings mainly depends on the joints configuration. Packing materials are placed in circumferential joints in order to properly transfer the longitudinal advance force of the TBM through the rings and to regularize the contact surface (Fig. 1). Packers are usually made of wood or plastic compounds and present a small thickness (around 2 mm). The majority of the tunnel projects present a planar configuration of the circumferential joints and, therefore, the force transferences between rings are exclusively performed through the packers. The structural interaction in front of radial loads is therefore conditioned by the tangential force capacity of the packer-concrete pack, which response is clearly determined by a frictional mechanism. The normal stress presented at packers due to the applied longitudinal force, determines the tangential capacity of the circumferential joint before its slipping. As a consequence, the assessment of the three dimensional response requires the consideration of the longitudinal force present at the lining [7,8]. Additionally, part of this force is progressively lost as time goes by due to the longitudinal creep of the lining [9]. Therefore, the structural interaction between adjacent rings can be modified with the aging of the structure.

A few tunnel projects, mainly subjected to bad soil conditions, include a dowel and socket system in order to limit the differences

\* Corresponding author. Tel.: +34 934017349; fax: +34 934054135.  
E-mail addresses: [oriol.arnau@upc.edu](mailto:oriol.arnau@upc.edu) (O. Arnau), [climent.molins@upc.edu](mailto:climent.molins@upc.edu) (C. Molins).

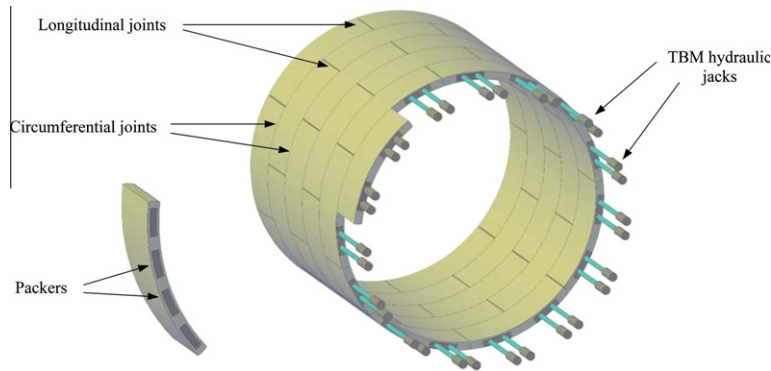


Fig. 1. Segmental tunnel lining.

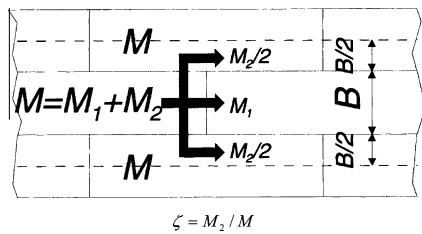


Fig. 2. Conceptual scheme of the bending forces transference ratio,  $\zeta$  [6].

joints present a complex **nonlinear** response caused by their incapacity of transferring tensile stresses, originating a gapping phenomenon from certain degree of rotation [2,12]. Their rotational response depends on the axial stress level, thus increasing the complexity of its appropriate consideration on the numerical models for structural analysis. As a consequence, it is necessary to employ advanced modeling procedures that include the accurate simulation of the joint behavior when the three dimensional response of a segmental tunnel lining is studied.

The present paper analyzes the influence of the interaction between adjacent rings in the structural response of segmental tunnel linings when they are subjected to typical design loads (longitudinally uniform). A theoretical analysis of the structural resistant mechanisms is carried out in order to establish the main parameters involved on the three dimensional response of the tunnel linings. A three dimensional finite elements model of a real tunnel section is performed, applying modeling techniques that allow the simulation of both the joints responses and the material behavior. A sensitivity analysis is performed in order to assess the influence of some parameters such as: the ground stiffness, the actual load and the remaining longitudinal force, on the three dimensional response of the structure. The results obtained allow to conclude about the influence of the main involved parameters and to determine the conditions in which coupling effects are relevant by comparing with the isolated ring results. The comparison of the results of the 3D model with those provided by common design simplifications illustrates the advantages and drawbacks of the latter, providing useful information for the design process of segmental tunnel linings.

## 2. Rings interaction mechanisms

When an individual ring is loaded (Fig. 3a), it deforms according to its flexibility until the ground provides the necessary reaction ( $F_{GR}$ ) to equilibrate the loads. The ground deformation to achieve such reaction depends on the surrounding ground stiffness and, therefore, it will play a decisive role on the radial displacements experienced by the ring (Fig. 3b).

Whilst concrete segments remain undamaged (with no cracks), the movements of the ring are mainly caused by concentrated rotations in longitudinal joints [13]. The contact zone of the longitudinal joints presents a smaller height than concrete segments, providing a lower mechanical inertia and hardly conditioning the flexibility of the ring. Additionally, the rotational stiffness of the longitudinal joints became severally reduced since gapping phenomenon occurs.

Fig. 3 shows the individual response of a ring in front of a localized load. In fact, the relative radial displacements between adjacent rings produce the shear deformation of the packers, orig-

in deformation between adjacent rings [2]. As a consequence, in dowel and socket joint, the packer only transfers tangential forces until the dimensional tolerance of the dowel and socket system is exhausted.

Some research programs have been developed in order to analyze the coupling effects on segmental tunnel linings subjected to longitudinally uniform design loads. Main conclusions pointed out the increase of the lining stiffness caused by coupling effects, reducing the experienced deformation and increasing the internal bending forces. Blom [2] developed an analytical model to study the effect of different circumferential joint stiffness for a certain tunnel case. He concluded that stiffer joints imply a significant increase of the ring internal bending forces (from 1.3 to 1.8 times the values obtained with the isolated ring) and a minor reduction on the movements, in comparison with those obtained by the isolated ring model. Klappers *et al.* [10] studied a particular tunnel configuration under longitudinally uniform design loads by using two different models: a 2D spring coupled beam model and a 3D shell elements FE model. The influence of different longitudinal force levels from 40 MN to 5 MN are analyzed through assuming a packer-concrete friction coefficient of  $\mu = 0.5$ , average value obtained in the tests performed by Gijssberg and Hordijk [11] on plywood packers. Klappers *et al.* [10] concluded that the real behavior of the joints must be taken into account within the structural analyses of segmental lining and, also, that the value of longitudinal force does not significantly influence the lining response. For uniform design loads, it is not necessary to employ a 3D model due to the similar results provided by the simplest beam spring model with coupled rings.

Despite the agreement in the significance of properly considering the longitudinal joints response, both Klappers *et al.* [10] and Blom [2] models use rotational springs to simulate the segments connection and analyze a unique and particular case of tunnel subjected to a unique load conditions. In fact, some segmental linings are analyzed by employing a rigid ring model, which stiffness is commonly reduced by means of the Muir-Wood formulation [1] in order to consider the longitudinal joints influence. Longitudinal

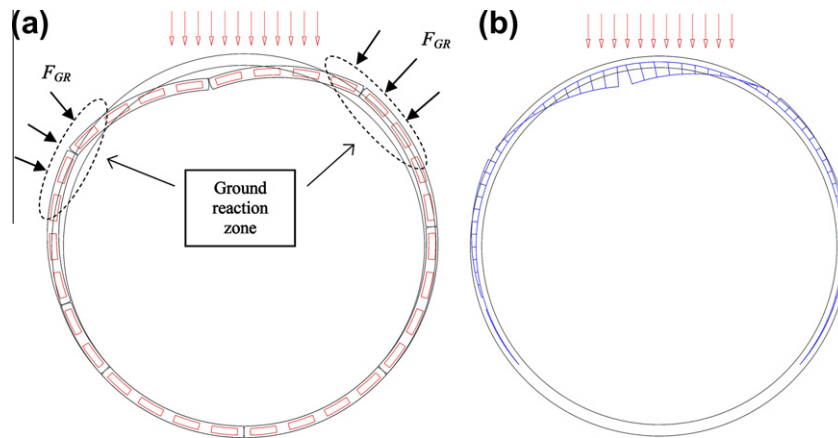


Fig. 3. Ring radial response mechanism (a) and displacement (b) in front of a localized load.

173 inating the transference of tangential forces between them. The  
174 shear response of the circumferential joints determines the struc-  
175 tural interaction between adjacent rings and, consequently, the  
176 degree of three-dimensionality of the lining behavior. Further  
177 reduction of the ground stiffness will result in higher differential  
178 radial displacements between adjacent rings, increasing the  
179 tangential force transferred and the influence of the structural  
180 interaction of rings.

181 Coupling effects can also influence the lining response when it  
182 is subjected to longitudinally uniform loads. The appliance of a  
183 perfectly hydrostatic pressure to a tunnel section (Fig. 4a) produces  
184 a pure compression state of the rings. Therefore, no movements are  
185 experienced in longitudinal joints and no interaction is expected  
186 between rings due to the same deformation of all of them. Commonly,  
187 the real pressure experienced by a tunnel is more similar  
188 to Fig. 4b, presenting differences between the vertical and the hori-  
189 zontal pressure due to the ground mechanical response. The resis-  
190 tance of this load unbalance requires the ovalization of the ring in  
191 order to find the necessary ground reaction to equilibrate the load.  
192 Different radial positions of the longitudinal joints between adja-  
193 cent rings produce small differences in their deformations  
194 (Fig. 5a). As a consequence, relative radial displacements occur  
195 between adjacent rings (Fig. 5b), activating the tangential force  
196 transference mechanisms and modifying the expected structural  
197 response of an isolated ring.

198 Load unbalance cannot be directly analyzed as the difference  
199 between the maximum and the minimum pressures. The

longitudinal joints response depends on the circumferential  
compression of the ring and, therefore, the load unbalance has to  
be related to the general magnitude of the load. In the present pa-  
per, the load unbalance is analyzed by means of Eq. (1) (ovalization  
load, OVL), which describes the difference between the mid tunnel  
horizontal pressure and the crown vertical pressure in respect to  
the last one (Fig. 4b).

$$OVL = \frac{P_{v,top} - P_{h,side}}{P_{v,top}} (\%) \quad (1)$$

In summary, the most influencing parameters on the coupling  
effect for a certain structure configuration would be the ground  
stiffness and the unbalance of the ground load. Additionally, the  
longitudinal force present at the lining has to be also considered  
due to its influence on the capacity of the circumferential joints  
to transfer shear loads between adjacent rings.

### 3. Rings interaction under design loads

The present section analyzes the structural response of the lin-  
ing when it is subjected to design loads (longitudinally uniform).  
The main objective is the analysis of the most important param-  
eters involved in the coupling effects in order to determine its influ-  
ence on the lining response. An advanced 3D FE model of a real  
section composed of eleven rings is developed to adequately repro-  
duce the lateral interaction between adjacent rings. Results are

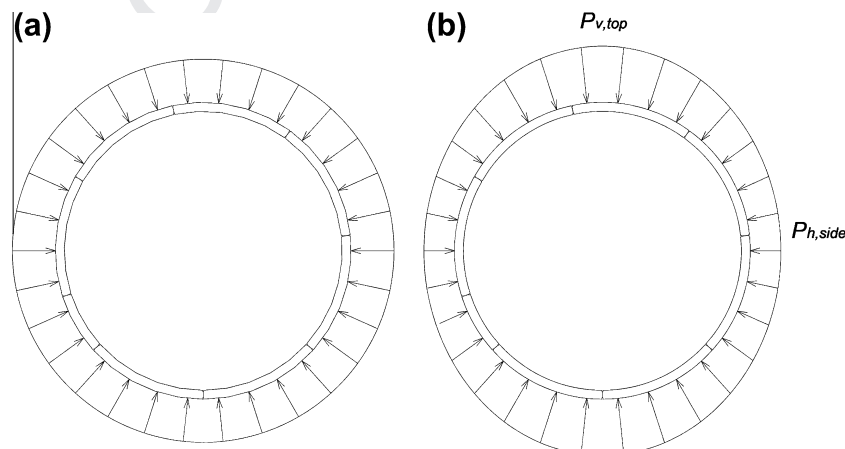


Fig. 4. Perfectly hydrostatic pressure (a) and tunnel typical external pressure (b).

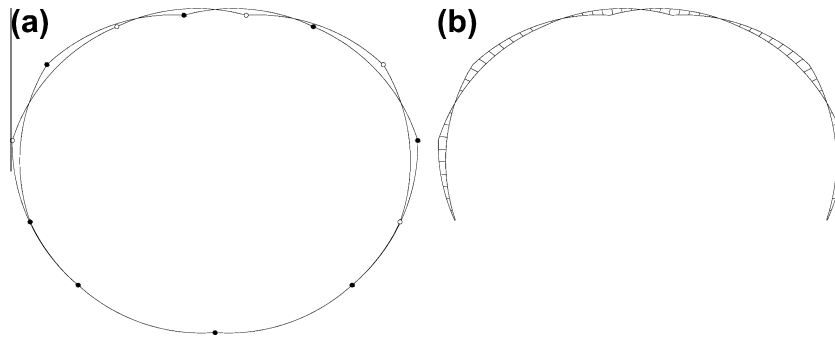


Fig. 5. Different deformation of two adjacent rings subjected to the load pattern of Fig. 4b (a) and the resulting radial relative displacements (b).

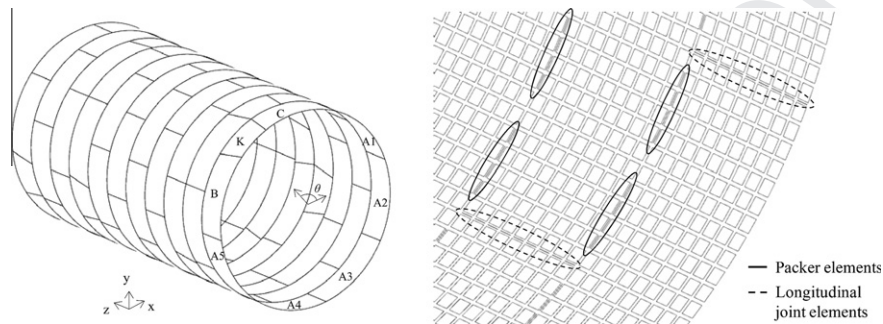


Fig. 6. 11 Rings numerical model of L9 section.

Table 1  
K segment positions of the modeled section of Line 9 tunnel.

Modeled ring number	1	2	3	4	5	6	7	8	9	10	11
K angular position, $\theta$ (°)	138	114	234	354	18	306	66	210	90	282	210
Z initial (mm)	0	1802	3604	5406	7208	9010	10812	12614	14416	16218	18020
Z final (mm)	1800	3602	5404	7206	9008	10810	12612	14414	16216	18018	19820

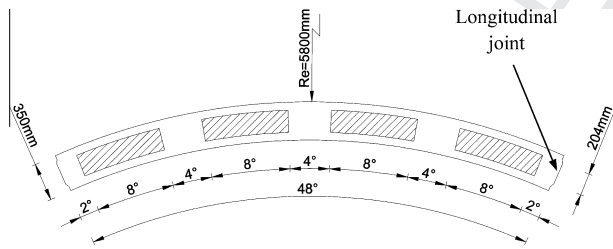


Fig. 7. Packers configuration of L9 circumferential joint.

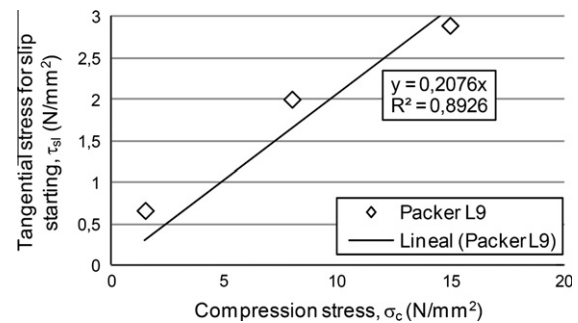


Fig. 8. L9 packer-concrete friction coefficient obtained from the test performed by Cavalero [14].

224 compared with those obtained in an isolated ring model, showing  
225 the significance of the coupling effects on the segmental tunnel linings  
226 structural response.

227 3.1. Case study and model description

228 In order to perform the study on a real structure, a section of  
229 eleven rings of Line 9 (L9) subway tunnel of Barcelona is modeled  
230 (Fig. 6). These rings are composed by seven conventional segments  
231 (A, B and C) plus 1 key segment (K), with an external diameter of  
232 11.6 m, 0.35 m thickness, 1.80 m width and 0.57° conicity [13].  
233 The particular location of the K segment in each ring is reproduced  
234 in the model (view Table 1).

235 Every concrete segment is modeled by means of 216 4-node  
236 quadrilateral shell elements (and 108 in the K segments due to

Table 2  
Finite elements types and characteristics employed in the numerical analyses.

	Description	Quantity
Nodes		20680
Segments elements	Quadrilateral 4 nodes curved shell elements	17820
Packer elements	Line interface shell elements, 2 + 2 nodes	1200
Segment joints elements	Line interface shell elements, 2 + 2 nodes	792
Spring elements	Translation spring element, 1 node	62040

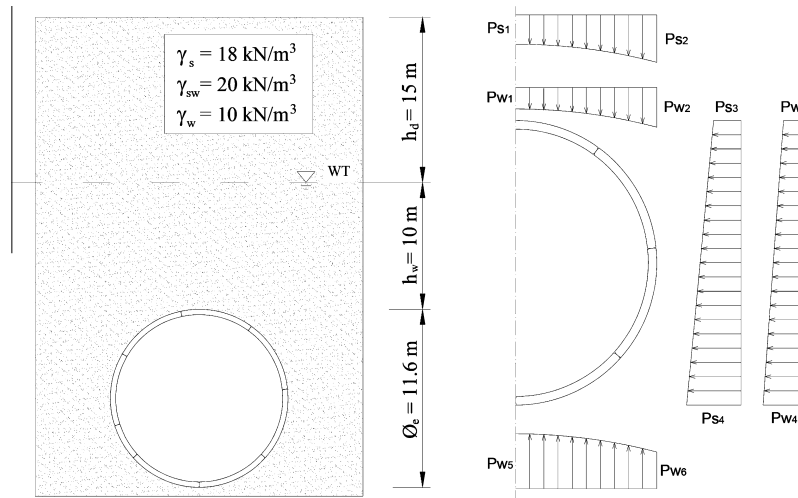


Fig. 9. Analyzed tunnel scenario and associated ground loads over L9 structure.

Table 3  
Values for performing the parametric analysis.

Property	Values
Ground modulus of elasticity, $E_s$ (N/mm <sup>2</sup> )	25–50–75–100–125–150
Lateral earth pressure, $K_0$	0.2–0.3–0.4–0.5–0.6
Correspondent ovalization load, OVL (%)	48.2–39.1–30–20.8–11.7
Longitudinal force, $N$ (MN)	40, 32, 24, 16, 8, 4
Total amount of cases	180

its reduced size). Initial model assumes a concrete linear behavior, presenting an elastic modulus of 38.700 N/mm<sup>2</sup> and a Poisson ratio of 0.2. In some of the analysis (Section 3.3), a more realistic material behavior of reinforced concrete is considered, including both cracking in tension and crushing in compression for the concrete and yielding of the steel reinforcement bars.

Longitudinal joints (between segments of a same ring, Fig. 1) present a concrete to concrete contact surface of 204 mm height (Fig. 7). Nonlinear interface elements with eleven integration points along their thickness (height of the joint) are employed to connect the shell elements of the segments (Fig. 6), behaving rigid in compression whilst gapping is produced in tension to reproduce the joint opening [12].

Circumferential joints (between adjacent rings, Fig. 1) are composed by a total amount of 30 plastic packers of 2 mm in thick. Each packer presents the same height of the longitudinal joint (204 mm) and encompasses an angle of 8°, defining the lateral configuration of the segment that is presented in Fig. 7 (except for K segment which only encompasses 2 packers). Every packer is modeled through the same interface elements used in longitudinal joints, connecting the shell elements of concrete segments at the actual positions of the packers (Fig. 6). The reproduction of the frictional response presented by the packer-concrete contact is performed by means of a Mohr–Coulomb constitutive equation, which also includes gapping in tension. The elastic properties of the packer are an elastic modulus ( $E_p$ ) of 202.1 N/mm<sup>2</sup> [9] and a shear modulus ( $G_p$ ) 77.7 N/mm<sup>2</sup>. The determination of the friction coefficient is based on the tangential resistance tests performed by Cavalaro [14] on L9 packer at three different normal stresses. The linear regression of the tangential stress values that produce the slipping of the packer provide the friction coefficient to take into account in the model,  $\mu = 0.2076$  (Fig. 8). A gap formation value of 0.278 N/mm<sup>2</sup> is assumed in order to consider the small joint pre-stressing originated by the tightening of the provisional steel bolts

employed during the ring erection process. The influence of the waterproof gaskets is not considered.

The ground–structure interaction is modeled by means of spring elements placed in radial, tangential and longitudinal directions [7,12,15], defining the boundary conditions of the analyzed numerical model. Unilateral response is assigned to radial springs in order to allow the loose of contact with the ground, determining its stiffness ( $K_r$ ) according to Eq. (2), which corresponds to the analytical solution of a circular tunnel in elastic ground ( $R$  define the tunnel radius and  $E_s$  the ground modulus of elasticity). Tangential ( $K_t$ ) and longitudinal ( $K_l$ ) stiffness (Eqs. (3) and (4)) are assumed as 1/3 of the radial one [13], assuming a Poisson ratio of  $\nu = 0.3$ . The description and the amount of finite elements used in the three dimensional model are shown in Table 2.

$$K_r = \frac{E_s}{R \cdot (1 + \nu)} \quad (2)$$

$$K_t = \frac{K_r}{3} \quad (3)$$

$$K_l = \frac{K_r}{3} \quad (4)$$

The tunnel scenario presented in Fig. 9 is employed to determine the design loads of the case study according to Eqs. (5)–(11). The tunnel crown presents an overburden of 25 m whilst the groundwater table is located 15 m below the surface. The ground presents a common density of  $\gamma_s = 18$  kN/m<sup>3</sup> which is converted to  $\gamma_{sw} = 20$  kN/m<sup>3</sup> when it becomes saturated of water ( $\gamma_w = 10$  kN/m<sup>3</sup>).

$$Ps_1 = h_d \cdot \gamma_s + h_w \cdot (\gamma_{sw} - \gamma_w) \quad (5)$$

$$Ps_2 = h_d \cdot \gamma_s + (h_w + \Phi_e/2) \cdot (\gamma_{sw} - \gamma_w) \quad (6)$$

$$Ps_3 = Ps_1 \cdot K_0 \quad (7)$$

$$Ps_4 = [h_d \cdot \gamma_s + (h_w + \Phi_e) \cdot (\gamma_{sw} - \gamma_w)] \cdot K_0 \quad (8)$$

$$Pw_1 = Pw_3 = h_w \cdot \gamma_w \quad (9)$$

$$Pw_2 = Pw_6 = (h_w + \Phi_e/2) \cdot \gamma_w \quad (10)$$

$$Pw_4 = Pw_5 = (h_w + \Phi_e) \cdot \gamma_w \quad (11)$$

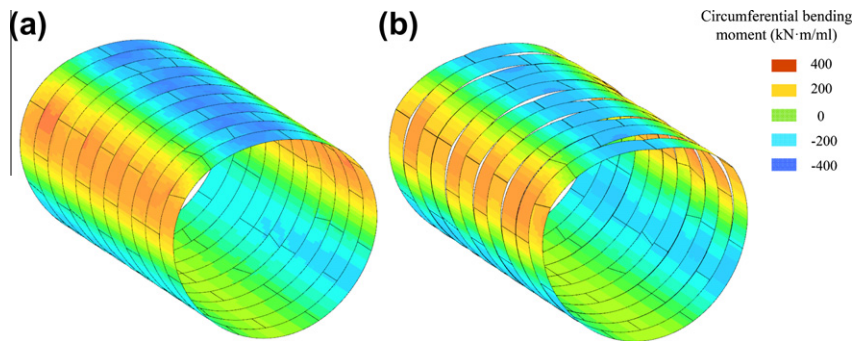


Fig. 10. L9 Deformation and circumferential bending moment for  $E_s = 25 \text{ MPa}$ ,  $K_0 = 0.5$  for the coupled system ( $F = 40 \text{ MN}$ ) (a) and uncoupled (b) (deformation amplification factor = 18).

In order to analyze the influence of the load unbalance, the ground modulus of elasticity and the longitudinal force in the coupling effects, a comprehensive parametric analysis is performed using the three dimensional model. The ground lateral earth pressure ( $K_0$ ) varies from 0.6 to 0.2 to define the range of ovalization loads (Table 3) – the ground modulus of elasticity ( $E_s$ ) is varied from 25 MPa to 150 MPa – coupling effects are negligible for higher values of  $E_s$ , and six different values of the longitudinal force ( $N$ ) from 40 MN to 4 MN are considered (view Table 3). The combination of these parameters generates a total amount of 180 cases.

The adequate reproduction of the tunnel loading requires two different steps in the numerical model. Firstly, the longitudinal force is applied at both sides of the model, deactivating the ground-structure interaction in order to generate the initial longitudinal compression of the section, as occurs after assembling the rings inside the shield of the TBM. Then, the ground-structure is fully activated and the ground pressure is applied.

The lack of longitudinal force (0 MN case) is considered as an isolated ring because coupling effects are then negligible. The central ring of the section (number 6 in Table 1) is employed to determine the structure response in such conditions.

The longitudinal force is a time dependant parameter due to its progressive reduction caused by lining creep. A comprehensive explanation of the phenomenon and a procedure to estimate the

time evolution of the longitudinal force are presented in Arnau et al. [9]. In the present study, time is not considered as a varying parameter and all analysis are developed in stationary conditions. Notice that the lining thickness of the case study could not be the optimal for some of the planned cases (i.e. for really soft grounds and high unbalanced loads it should be larger). However, it is necessary to assume a unique standard to properly contrast the results, and Line 9 provides all the data required for this application.

3.2. Results

Coupling effects produce that the radial displacement differences between adjacent rings originated by the staggered configuration of the joints is diminished, providing a stiffer response of the lining (Fig. 10). As a consequence, the global deformation of the lining is reduced whilst the internal bending forces increase.

The study of the coupling effects influence on the lining deformation is carried out by analyzing the vertical ovalization of the central ring of the section (ring 6), defined as the difference between the vertical displacement on the top and the bottom of the ring. The effects on the internal forces are determined by analyzing the circumferential bending moments at the same central ring, which common response can be observed in Fig. 11.

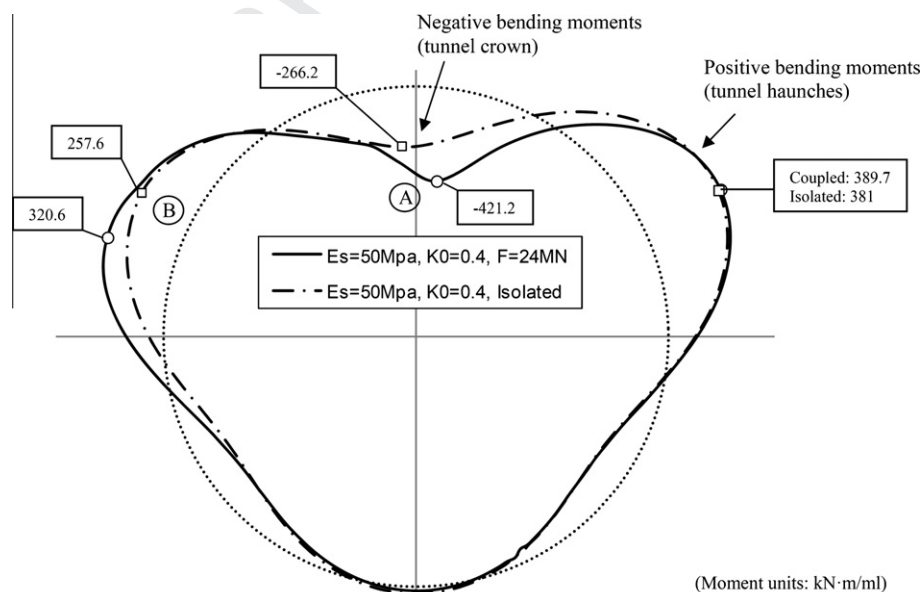


Fig. 11. Representation of the circumferential bending moment of the central ring (6) for  $E_s = 50 \text{ MPa}$  and  $K_0 = 0.4$  in the coupled system ( $F = 24 \text{ MN}$ ) and in the isolated ring.

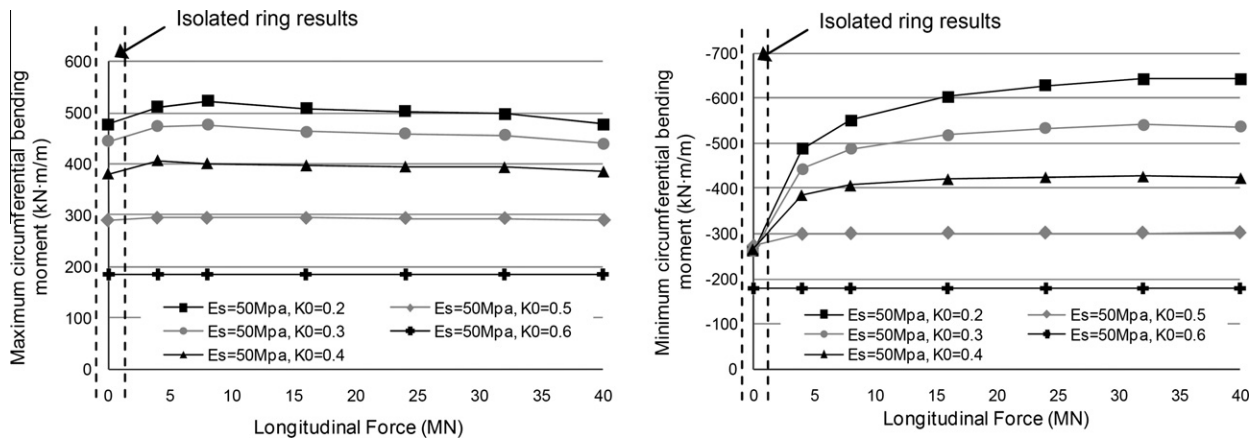


Fig. 12. Maximum (positive) and minimum (negative) values of the internal bending forces for the central ring of the section (ring 6) for the case of  $E_s = 50$  MPa.

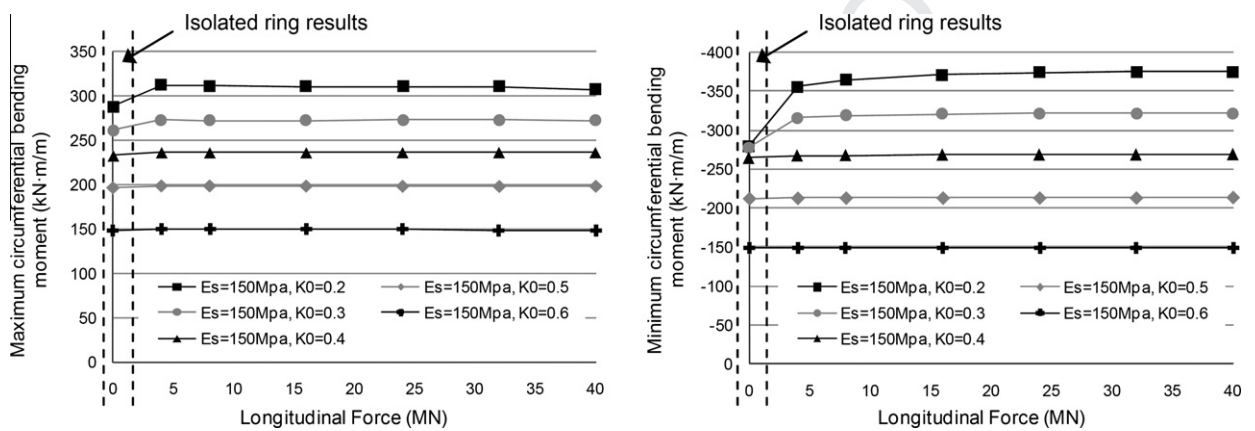


Fig. 13. Maximum values of the internal bending forces for the central ring of the section (ring 6) for the case of  $E_s = 150$  MPa.

Maximum positive bending moments are produced in the haunches of the arch defined by the upper half of the ring whilst maximum negative bending forces are located close to the tunnel crown. Fig. 11 clearly shows the local increase of the circumferential bending moments caused by the adjacent rings deformations. Points A and B correspond to the positions where the radial displacement difference and the consequent tangential force are maximum, clearly denoting the position of the adjacent rings longitudinal joints.

The numerical results of the maximum and minimum circumferential bending moments with a ground stiffness of 50 MPa are presented in Fig. 12. As can be observed, the increase of the ovalization load (decrease of  $K_0$ ) implies the production of higher bending forces at the tunnel crown zone with respect to the isolated ring results, achieving a maximum increase of 146% for  $K_0 = 0.2$  and 59% for  $K_0 = 0.4$ . The presence of a small longitudinal force is enough to produce coupling effects, which appear to be independent of the force magnitude out of high ovalization loads. For low ovalization load, ( $E_s = 50$ ,  $K_0 = 0.6$ ) the coupling effects are not presented, obtaining the same results than in the isolated ring for all longitudinal forces.

Contrarily, the maximum positive bending forces produced at the upper haunches of the tunnel do not show significant differences in all cases. Despite the difference in shape shown in the left haunch of Fig. 11, maximum values do not present differences respect to the isolated ring model due to their allocation on the stiffer haunch depending on the longitudinal joints positions.

For  $E_s = 50$  MPa, the isolated ring analyses provide similar crown bending forces for the majority of ovalization loads. This fact is caused by the exhaustion of the upper longitudinal joints capacity, increasing the obtained movements and presenting larger differences respect to the coupled analysis as  $K_0$  value decreases.

The analysis of the ground stiffness  $E_s = 150$  MPa (Fig. 13) reveals that coupling effects are only presented for  $K_0 = 0.2$  and  $K_0 = 0.3$ , showing increases of the crown bending moment of 34% and 16% respectively. As a consequence, stiffer ground conditions reduce the influence of the coupling effects, increasing the necessary ovalization loads to produce it, and diminishing its influence on the lining internal forces.

The influence of the ground stiffness can be more accurately appraised in Fig. 14, where the increase of the tunnel crown bending forces and the reduction of the vertical ovalization respect to the isolated ring results are depicted. As can be observed, the consideration of the coupling effects only presents a significant influence on the obtained results when the segmental lining is analyzed in really soft ground conditions or for significant ovalization loads. For  $K_0 = 0.5$ , the coupling effect only influences the results for ground stiffness under 75 MPa, but for  $K_0 = 0.3$ , significant influences are obtained until  $E_s = 150$  MPa. The combination of both factors provides the highest coupled scenario, obtaining increments of bending forces up to 180% respect of the isolated ring for  $E_s = 25$  MPa and  $K_0 = 0.3$ .

Coupling effects also influence the deformations of segmental linings (Fig. 14). Reductions between 15% and 25% of the central

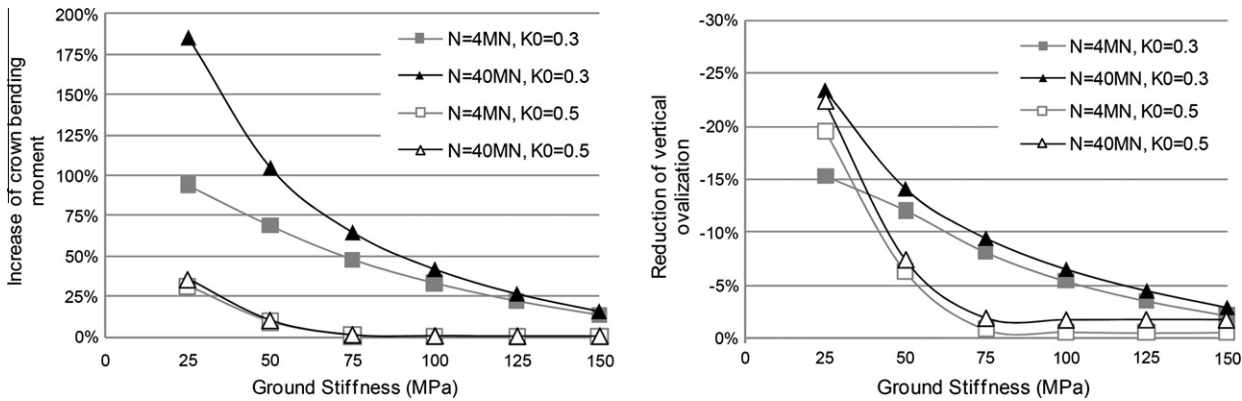


Fig. 14. Influence of coupling effects respect to the isolated ring results.

ring vertical ovalization are obtained for really soft grounds, denoting the increase of the lining stiffness respect of the isolated ring consideration.

The diminution of the longitudinal force produces that the slipping of the packers starts for a lower tangential force. As a consequence, coupling effects are diminished, reducing the increase of the internal forces and providing larger lining deformations (Fig. 14). Despite that, significant influences of the longitudinal force magnitude are only presented for extremely soft ground and high ovalization pressures.

The sensitivity analysis allows the determination of the ground stiffness and ovalization loads in which coupling effects play a significant role for the case study. The coupling influence zone (Fig. 15) determines the conditions where differences over 10% are obtained in vertical ovalization and bending moment respect to the isolated ring results. The longitudinal force value only presents influence when the reduction of vertical ovalization is considered.

These results are obtained for the rings configuration of Table 1 compared with those provided by the isolated ring 6. Coupling effects produce that the lining behave more similar to a rigid pipe and, consequently, no significant differences are expected in respect to other sections of the same tunnel with different positions of the longitudinal joints caused by different rings configurations (K segment position, Fig. 6).

Segmental tunnel linings are confined in longitudinal direction by the surrounding ground. As a consequence, the radial loading of the rings can produce an increase of the longitudinal force of the lining due to the partial restraint of the transversal deformation (Poisson effect). For a certain ground load case, the circumferential

axial stress should be similar for all longitudinal forces and, therefore, presenting similar increments. The performed analyses show that for usual cases, stiffer ground conditions provide higher increases of the longitudinal force despite the obtained values are small, achieving a maximum of 0.42 MN for  $E_s = 150 \text{ N/mm}^2$  (Fig. 16). Cases with reduced initial longitudinal force and significant rings deformations (combination of reduced ground stiffness and high ovalization loads), can present higher increments of the longitudinal force (Fig. 16). This fact should be caused by movements of the rings that originate the dislocation of the segments, producing a small plane arch mechanism.

### 3.3. Influence of lining slenderness and longitudinal joints relative height

The magnitude of the displacements experienced by a certain ring also depends on its flexibility. More rigid rings imply lower deformations and, therefore, a reduced influence of the coupling effects is initially expected. Segmental tunnel lining of Line 9 presents a small thickness ( $e$ ) of 350 mm in front of its big internal diameter ( $\Phi_i$ ) of 10.9 m, defining a high slenderness ratio ( $Sl = \Phi_i / e$ ) of 31.1 with respect to similar structures. In order to analyze the relation between the coupling effects and the linings flexibility, different slenderness ratios from 31.1 to 17.8 are analyzed on the previously described 3D model (Table 4).

The numerical study is based on the scenario defined by a ground elasticity modulus of  $E_s = 25 \text{ N/mm}^2$ , a lateral earth pressure coefficient  $K_0 = 0.5$  and the maximum longitudinal force of 40 MN. Table 4 shows the lining configurations analyzed and the correspondent lining slenderness, respecting the proportion

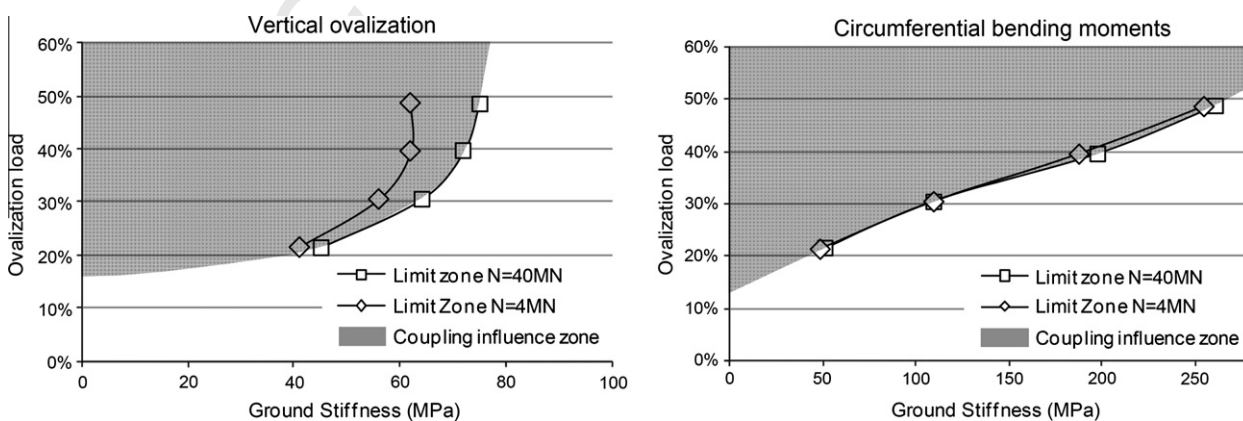


Fig. 15. Coupling influence zones for deformation and circumferential bending moment.

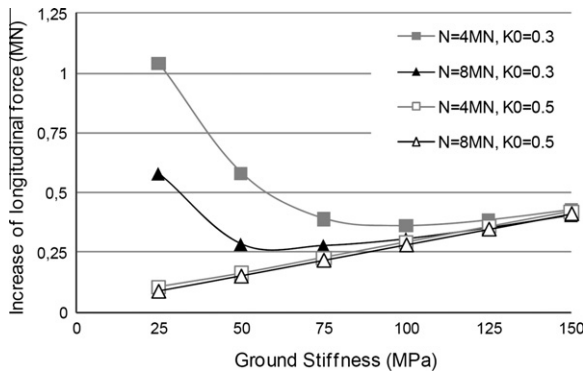


Fig. 16. Increase of the longitudinal force caused by radial loading.

Table 4  
Cases used in the analysis of the influence of ring flexibility.

Case	Model diameter (mm)	Ring thickness, $e$ (mm)	Internal diameter, $\Phi_i$ (mm)	Slenderness, $Sl = \Phi_i/e$	Longitudinal joint height, $h_j$ (mm)
Line 9	11250	350	10900	31.1	204
SL-A	11250	400	10850	27.1	233
SL-B	11250	450	10500	24.0	262
SL-C	11250	500	10750	21.5	291
SL-D	11250	550	10700	19.5	321
SL-E	11250	600	10650	17.8	350

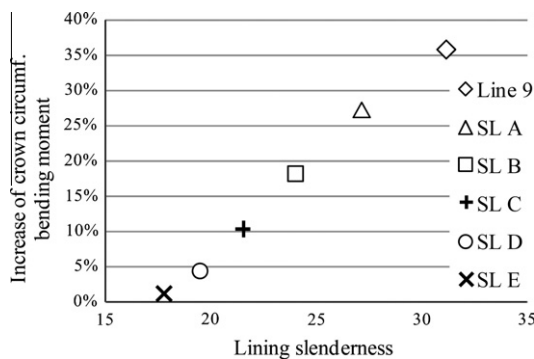


Fig. 17. Influence of coupling effects with respect to lining stiffness (central ring, 6). Case:  $E_s = 25$  MPa,  $K_0 = 0.5$  and  $F = 40$  MN.

between the segment thickness and the longitudinal joint height defined in Line 9 configuration (Fig. 7). To exclusively analyze the influence of the lining slenderness, the configuration of joints between adjacent rings remains invariant and equal to described in Section 3.1. Isolated ring models of each case are also performed in order to determine the influence of the coupling effects.

Numerical results (Fig. 17) show that an increase of the lining slenderness implies a linear increase of the crown circumferential bending moment respect to the isolated ring approach. Therefore, the influence of coupling effects linearly increases with the growth of the linings slenderness.

As it is well known, the radial deformation of a ring is hardly influenced by the rotation of its longitudinal joints. Therefore, the flexibility of a segmental tunnel lining also depends on the relation between the segment thickness ( $e$ ) and the longitudinal joint height ( $h_j$ ) (Fig. 18), defined as the longitudinal joint relative height ( $e/h_j$ ). Reduced relative heights should imply higher concentrated rotations in joints, thus expecting higher influence of coupling effects.

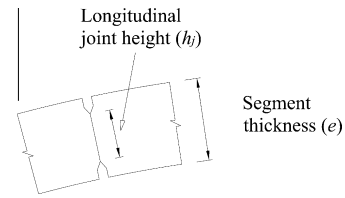


Fig. 18. Longitudinal joint scheme and nomenclature.

The 3D numerical model and scenario previously described for the analysis of slenderness influence is also used in order to analyze the influence of the longitudinal joint relative height in coupling effects. Four different relative heights, from 20% to 80%, are studied for two different linings slenderness (Table 5).

Numerical results show an exponential increase of the coupling effects with the decrease of the longitudinal joint relative height (Fig. 19). Higher slenderness of the lining implies lower influence of coupling effects, despite similar influence is also obtained for the lowest longitudinal joint relative height. According to the obtained results, maximize the longitudinal joint height implies a direct reduction of the influence of coupling effects.

### 3.4. Neglecting coupling effects

In Section 3.2 has been stated that bending forces obtained considering coupling effects can double the isolated ring approaches for soft ground conditions and high ovalization pressures. The structural design of segmental tunnel linings is commonly based on the isolated ring results and, therefore, it is necessary to determine the structural implications of neglecting coupling effects during the design process.

As can be expected, the increase of bending forces can achieve the cracking moment of the concrete section, producing changes in the stiffness of the structure and stress redistributions in this 3D system. In order to further analyze the structural response of the lining when cracking occurs, a nonlinear material version of the 3D model which properly considers the behavior of concrete and the reinforcement layout is developed. The Total Strain Rotate Crack model included in software Diana 9 is used, defining appropriate constitutive equations to simulate the reinforcement steel response, the concrete cracking in tension and its crushing in compression.

Two particular cases are analyzed;  $E_s = 50$  MPa -  $K_0 = 0.4$  and  $E_s = 25$  MPa -  $K_0 = 0.4$ . The results of the isolated ring models were used to determine the design internal forces (Table 6). The necessary amount of circumferential reinforcement for each case is determined by applying the Eurocode 2 regulations to the 350 mm height section (Table 6), presenting the symmetrical layout and the concrete cover of 50 mm shown in Fig. 20.

The reinforcement described in Table 6 and Fig. 20 is added to the 11 ring shell model by means of specific reinforcement elements, assigning them an elastic-plastic response with an elastic modulus of  $E_{steel} = 200$  GPa and a yield strength of  $f_y = 500$  N/mm<sup>2</sup>. The concrete behavior is assumed as elastic-plastic in compression and brittle in tension, presenting an elastic modulus of  $E_c = 38.7$  GPa, a compressive strength of 50 N/mm<sup>2</sup> and a tensile strength of 4.1 N/mm<sup>2</sup>. The analyses are performed progressively increasing the ground load for the maximum longitudinal force case (40 MN).

The analysis of the repercussions of neglecting coupling effects is performed through the comparison of the results obtained in the 3D nonlinear material model (NLM) with the results provided by the usual approaches employed on design processes. For such purpose, additional analyses using a continuous ring model were

**Table 5**  
Cases used in the analysis of the longitudinal joint relative height.

Case		Longitudinal joint relative height $e/h_j$ (%)	Ring thickness, $e$ (mm)	Longitudinal joint height, $h_j$ (mm)
Based on L9 slenderness	Line 9	58.3	350	204
	Joint I	20	350	70
	Joint II	40	350	140
	Joint III	80	350	280*
Based on SL-C slenderness	Line 9	58.3	500	291
	Joint I	20	500	100
	Joint II	40	500	200
	Joint III	80	500	400

\* Unrealistic case for pressuring concrete out of the reinforcement zone (concrete cover).

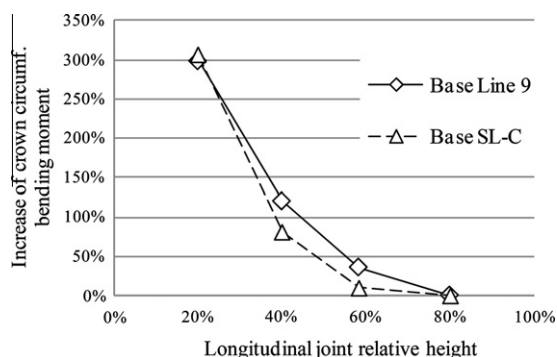


**Fig. 19.** Influence of coupling effects respect to the longitudinal joint relative height (central ring, 6). Case:  $E_s = 25$  MPa,  $K_0 = 0.5$  and  $F = 40$  MN.

**Table 6**  
Design internal forces and obtained reinforcement for nonlinear material analyses.

Case	Design axial force, $N_d$ (kN/m)	Design bending force, $M_d$ (kN m/m)	Reinforcement (both sides)
$E_s = 50, K_0 = 0.4$	3975	571.5	5 $\phi$ 20 per meter
$E_s = 25, K_0 = 0.4$	4035	664.05	5 $\phi$ 25 per meter

carried out, both considering the full thickness of the lining (Rigid) and also reducing its inertia according to the formulation proposed by Muir-Wood [1] (Eq. (12)), where  $I$  and  $I_j$  represent the segment and longitudinal joint inertia respectively, whilst  $n$  define the number of joints of the ring.

$$I_e = I_j + I \cdot \left(\frac{4}{n}\right)^2 \quad (12)$$

The increase of the internal bending forces caused by coupling effects produces the concrete cracking on both cases, as can be clearly appraised in Figs. 21–23 by the sudden separation of the linear response. This phenomenon implies a reduction of the lining stiffness, obtaining an increase of the central ring ovalization (Fig. 21). As a consequence, the isolated ring results and the Muir-Wood results present a good agreement with the expected deformation. The Rigid approach presents similar deformations than linear 3D model, according to the increase of the stiffness provided by the coupling effects.

Segments cracking produce redistributions of the bending moments, originating the diminution of the maximum and minimum values achieved (Figs. 22 and 23). The isolated ring results provide good general results with a slight underestimation of maximum negative bending moment, showing that certain degree of interaction remains in the structure despite segments cracking. According to that, favorable conditions for coupling effects (reduction of ground stiffness) imply an increase of the isolated ring approach

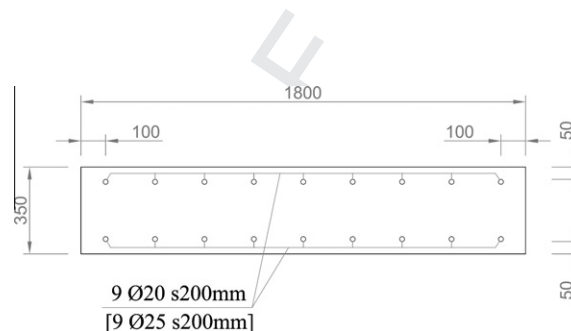


**Fig. 20.** Layout of the circumferential reinforcement for nonlinear analyses.

deviation (Fig. 23). Muir-Wood results present an excellent agreement to the maximum negative bending moments for both cases but present significant differences for positive bending moments. This fact is caused by the assumption of a general diminished inertia, do not considering that joints close to the tunnel crown present more influence due to the applied load profile.

The analysis of the reinforcement tensile stress (Fig. 24) reveals that maximum values, and the consequent maximum crack widths, are presented in the laterals of the segments, where the tangential forces are transferred, diminishing with their advance to the center of the segments (Fig. 24).

The stress states of the segments and the reinforcements are employed to determine the maximum crack widths according to Eurocode 2 regulations (Table 7). Despite the significant influence that coupling effects present on the elastic internal forces of the lining, sections designed from the isolated ring results present crack widths inside the limits recommended by Eurocode 2 to accomplish the serviceability limit state. As it is shown in Table 7, a maximum crack width of 0.2 mm is numerically obtained, in front of the maximum of 0.3 mm recommended by Eurocode 2 for the most restrictive exposure class. Therefore, the consequences of employ an isolated ring model in the structural design of segmental tunnel linings should be acceptable out of extreme unfavorable conditions.

In summary, the 3D nonlinear material analysis reveals that

- The employment of an isolated ring model including longitudinal joints provides an underestimation of the internal bending forces, denoting that coupling effects still produce an increase of the lining stiffness despite the cracking of the segments. On the other hand, it was stated that the employment of the isolated ring results to design the lining reinforcement, should provide enough resistance to maintain crack widths inside the limits fixed by concrete codes for the serviceability state.
- The isolated rigid ring model, disregarding joints effects, presents a very good agreement in respect to the linear coupled analysis of the lining, clearly showing the inhibition of the longitudinal joints caused by coupling effects. As a consequence, the isolated rigid ring model could be useful to analyze

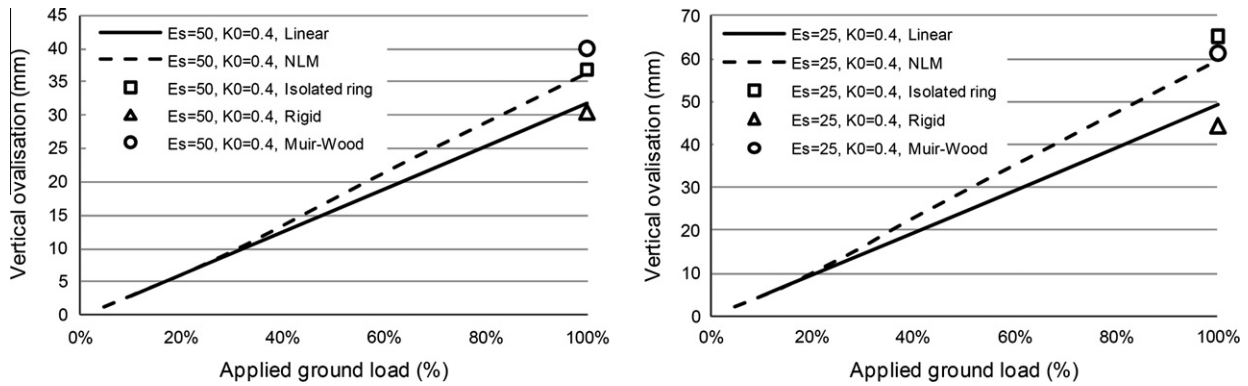


Fig. 21. Vertical ovalization of central ring (6) obtained with different numerical approaches.

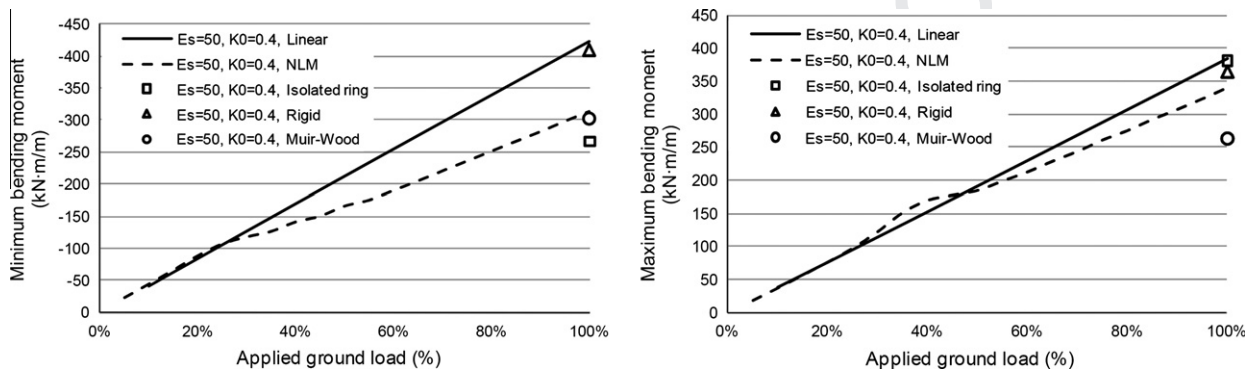


Fig. 22. Central ring (6) maximum bending forces obtained with different numerical approaches ( $E_s = 50, K_0 = 0.4$ ).

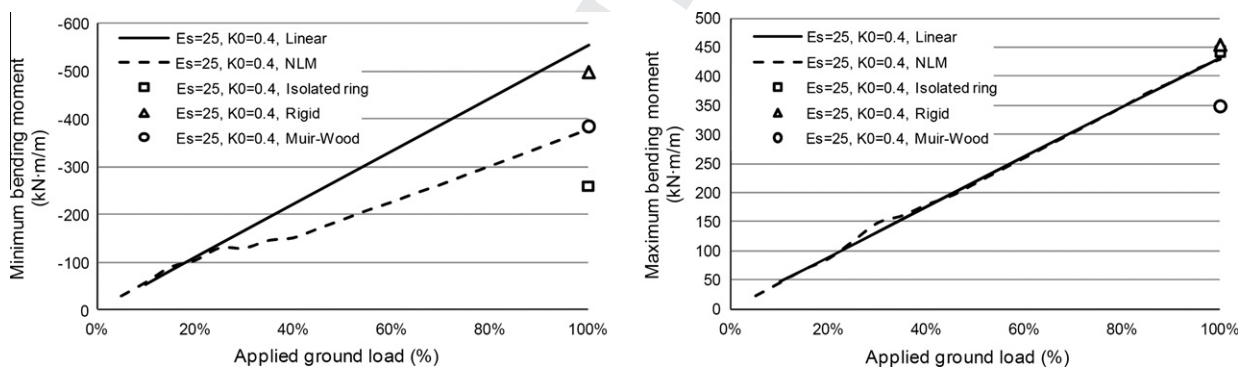


Fig. 23. Central ring (6) maximum bending forces obtained with different numerical approaches ( $E_s = 25, K_0 = 0.4$ ).

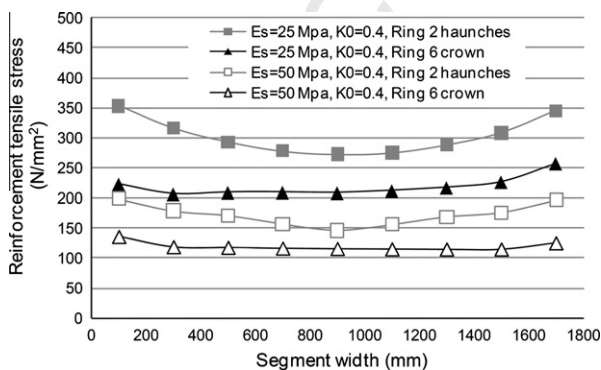


Fig. 24. Reinforcement tension stress distribution across the section with the maximum crack opening (haunches of ring 2) and across the crown of the central ring (6).

Table 7  
Crack widths ( $w_m$ ) obtained at the nonlinear material analyses of the lining section.

Case	Central ring crown crack width (mm)	Maximum crack openings (mm)		
		Position	Center of the segment	Lateral of the segment
$E_s = 50, K_0 = 0.4$	0.08	Ring 2 haunches		0.11
$E_s = 25, K_0 = 0.4$	0.12	Ring 2 haunches		0.15
	0.2			

cases affected by coupling effects but where segment's cracking is not achieved. In the case that loading produce cracking, rigid isolated ring provides an upper bound of the extreme bending forces, placing its employment for design purposes on the safety side.

- The reduction of rigid ring inertia proposed by Muir-Wood [1] is uniformly applied to the whole ring, do not considering the fact that certain joints present more influence than others due to the load profile. As a consequence, very good agreement has been obtained in some results (displacements and negative bending moments) whilst a significant underestimation of the maximum bending moment is detected.

#### 4. Conclusions

When a segmental tunnel lining is subjected to a longitudinally distributed design loads, the staggered configuration of its joints produces the activation of force interaction mechanisms between adjacent rings, originating the so called coupling effects. As a consequence, the lining behaves as a 3D structure, presenting an increase of its stiffness and internal forces in respect to the isolated ring consideration.

The analysis of the lining radial response and the force transmission mechanisms between adjacent rings determines that, for certain segmental lining configuration (thickness, joints positions and height, packer materials, etc.) ground stiffness, load unbalance and longitudinal force should be the most influence parameters in the coupling effects.

Results of the sensitivity analyses reveal that coupling effects are significant when the lining is embedded in soft ground conditions (below  $E_s = 150$  MPa in the case study) or subjected to high unbalanced loads. Coupling effects produce a significant increase in lining radial bending forces respect to the isolated ring consideration, achieving on the case study increases over 150% for unfavorable conditions. The lining deformation is also reduced but in a minor significance, presenting maximum reductions of the vertical ovalization around 25%.

The necessary longitudinal force level to develop coupling effects is small compared with the usual forces exerted by the TBMs during the tunnel construction. As a consequence, the magnitude of the longitudinal force does not significantly influence the structural response of the lining out of the combination of really soft grounds and high unbalanced loads.

Coupling effects present a significant sensitivity to the radial flexibility of segmental tunnel linings. For a certain circumferential joint configuration, the increase of the lining slenderness produces a linear increase on the influence of coupling effects, whenever the proportion between the linings thickness and the longitudinal joint height is maintained. Similarly, increase the lining flexibility by reducing the ratio between the longitudinal joint height and the thickness of the segments produce an exponential increase of the influence of coupling effects. As a consequence, maximize the height of the longitudinal joints will reduce the significance of coupling effects in the structural response of segmental tunnel linings.

The structural design of segmental tunnel linings is commonly tackled by means of isolated ring approaches and, therefore, it is necessary to determine the influence of neglecting the coupling effects. The increase of the internal forces generated by coupling effects can produce the segments cracking, reducing the lining stiffness and behaving in between a rigid pipe and an isolated ring. The employment of the isolated rigid ring model arises as a design option that provide an upper bond for the internal bending forces when coupling effects influences the segmental lining response.

#### Acknowledgements

The authors want to thank the construction company FCC Construcción, S.A. for its involvement in the research of the structural response of segmental tunnel linings through the research program *Túneles Urbanos*. The first author also wants to thank the support of the University and Research Commissioner of the DIUE of the Generalitat de Catalunya and also the European Social Fund (ESF).

#### References

- [1] Muir Wood AM. The circular tunnel in elastic ground. *Géotechnique* 1975;25(1):115–27.
- [2] Blom, C.B.M., 2002. Design philosophy of concrete linings for tunnels in soft soils. PhD thesis. Technische Universiteit Delft.
- [3] Teachavorasinskun S, Chub-uppakarn T. Influence of segmental joints on tunnel lining. *Tunn Undergr Space Technol* 2010;25:490–4.
- [4] Guglielmetti V, Grasso P, Mahtab A, Xu S. Mechanized tunnelling in urban areas. London: Taylor & Francis; 2008.
- [5] Japan Society of Civil Engineers (JSCE). Japanese standard for shield tunneling; 1996.
- [6] Koyama Y. Present status and technology of shield tunnelling method in Japan. *Tunn Undergr Space Technol* 2003(18):145–59.
- [7] Blom CBM, van der Horst EJ, Jovanovic PS. Three-dimensional Structural Analyses of the shield-driven “Green Heart” tunnel of the high-speed line south. *Tunn Undergr Space Technol* 1999;1(2):217–24.
- [8] Mo HH, Chen JS. Study on inner force and dislocation of segments caused by shield machine attitude. *Tunn Undergr Space Technol* 2008;23:281–91.
- [9] Arnau O, Molins C, Blom CBM, Walraven JC. Longitudinal-time dependent response of segmental tunnel linings. *Tunn Undergr Space Technol* 2012;2(28):98–108.
- [10] Klappers C, Grübl F, Ostermeier B. 2006. Structural analyses of segmental lining – coupled beam and spring analyses versus 3D-FEM calculations with shell elements. In: Proceedings of the ITA-AITES 2006 world tunnel congress, safety in the underground space. 6 pp.
- [11] Gijsberg FBJ, Hordijk DA. Experimenteel onderzoek naar het afschuifgedrag von ringvoegen. TNO-rapport COB K111; 1997 [in Dutch].
- [12] Arnau O, Molins C. Experimental and analytical study of the structural response of segmental tunnel linings based on an In situ loading test. Part 2: Numerical simulation. *Tunn Undergr Space Technol* 2011(26):778–88.
- [13] Molins C, Arnau O. Experimental and analytical study of the structural response of segmental tunnel linings based on an In situ loading test. Part 1: Test configuration and execution. *Tunn Undergr Space Technol* 2011;764–77.
- [14] Cavalero SHP. Aspectos tecnológicos de túneles construidos con tuneladora y dovelas prefabricadas de hormigón. PhD thesis. Universitat Politècnica de Catalunya; 2009 [in Spanish].
- [15] Plizzari GA, Tiberti G. Steel fibers as reinforcement for precast tunnel segments. In: Proceedings of the ITA-AITES 2006 world tunnel congress and 32nd ITA general assembly; 2006. 6 pp.